

# Nuclear Matter and Nuclear Dynamics

**M Colonna**

Laboratori Nazionali del Sud, INFN, via Santa Sofia 62, I-95123, Catania, Italy

E-mail: [colonna@lns.infn.it](mailto:colonna@lns.infn.it)

## 1. Introduction

The Equation of State (EOS) of nuclear matter plays a fundamental role in the understanding of many aspects of nuclear physics and astrophysics. Transient states of nuclear matter far from normal conditions can be created in terrestrial laboratories and many experimental and theoretical efforts have been devoted to the study of nuclear reactions, from low to intermediate energies, as a possible tool to learn about the behavior of nuclear matter and its EOS. In particular, the availability of exotic beams has opened the way to explore, in laboratory conditions, new aspects of nuclear structure and dynamics up to extreme ratios of neutron (N) to proton (Z) numbers. Over the past years, measurements of isoscalar collective vibrations, collective flows and meson production have contributed to constrain the EOS for symmetric matter for densities up to five times the saturation value [1]. However, the EOS of asymmetric matter has comparatively few experimental constraints: The isovector part of the nuclear effective interaction (Iso-EOS) and the corresponding symmetry energy are largely unknown far from normal density.

The knowledge of the EOS of asymmetric matter is very important at low densities, for studies concerning neutron skins, pigmy resonances, nuclear structure at the drip lines, neutron star formation and crust, as well as at high densities, for investigations of neutron star mass-radius relation, cooling, hybrid structure, transition to a deconfined phase, formation of black holes. Hence a large variety of phenomena, involving an enormous range of scales in size, characteristic time and energy, but all based on nuclear processes at fundamental level, are linked by the concept of EOS.

From one side, this has stimulated new thorough studies of the ground state energy of (asymmetric) nuclear systems, based on microscopic many-body approaches, from which EOS and effective interactions can be extracted, that are essential for modeling heavy ion collisions (HIC) and the structure of neutron stars [2, 3, 4, 5]. Predictions of different many-body techniques will be compared in Section 2.

On the other side, several observables which are sensitive to the Iso-EOS and testable experimentally, have been suggested [6, 7, 8, 9]. Taking advantage of new opportunities in theory (development of rather reliable microscopic transport codes for HIC) and in experiments (availability of very asymmetric radioactive beams, improved possibility of measuring event-by-event correlations), in the following Sections 3-5 we will review new studies aiming to constrain the existing effective interaction models. We will discuss dissipative collisions in a wide range of beam energies, from just above the Coulomb barrier up to the  $A\text{GeV}$  range. Low to Fermi energies will bring information on the symmetry term around (below) normal density, while intermediate energies will probe high density regions. As far as the high density behavior of asymmetric nuclear matter is concerned, neutron stars, where densities ten times higher than

the densities inside atomic nuclei may be reached in the core, appear as natural astrophysical laboratories that allow for a wide range of physical studies linked to the properties of ultra-dense matter and of its EOS. We will review recent developments in the field also in connection with the possibility that other degrees of freedom, besides the nucleonic ones, (hyperons, quarks), may appear, see Section 6. Finally, the link to the possible appearance of new phases of matter in charge asymmetric HIC, already at intermediate energies, is discussed in Section 7.

## 2. Nuclear matter EOS and microscopic approaches

The renewed interest in nuclear matter properties and EOS, that play an important role in the understanding of nuclear structure and astrophysical phenomena, has led to the development of more detailed investigations of the ground state of nuclear many-body systems, where the energy functional is evaluated starting from the bare nucleon-nucleon (NN) interaction. Therefore, from one side one is facing the problem of finding a fundamental scheme for the description of nuclear forces, valid from light nuclei up to dense matter, that is still an open fundamental problem, and, on the other, that of solving a complex many-body problem, that involves strongly spin-isospin dependent forces.

It is well known that all non-relativistic many-body theories need at least three-body forces (TBF) in the Hamiltonian. This is essential to reproduce the correct saturation point of the nuclear EOS, extracted from phenomenological data [10]. However, TBF cannot be constrained in a stringent way, due to the rather limited experimental data on three-nucleon systems. Phenomenological TBF have been devised to reproduce the properties of light nuclei and to correct the nuclear matter saturation point, leading to a new behavior of the whole EOS of both symmetric and asymmetric nuclear matter [11]. However, a unique TBF, which is able to describe accurately light nuclei, as well as the nuclear matter saturation point, is not available yet. Hence, it is interesting to study to which extent the nuclear matter EOS, in a wide density range, is actually dependent on the choice of two- and three-body forces, once the saturation point has been reproduced, i.e. to test to what extent the reproduction of the saturation point constrains the behavior of the whole EOS.

In the following we will review recent results obtained mostly in the context of the many-body Bethe-Brueckner-Goldstone (BBG) theory [4, 5], without the pretension to be exhaustive. Among the most accurate two-body forces, one has to consider the latest one of the Bonn potential series, that is more explicitly constructed from meson exchange processes [12]. Also the Argonne  $v_{18}$  NN interaction, that is constructed by a set of two-body operators which arise naturally in meson exchange processes, but with partially phenomenological form factors, can be considered as a very accurate one [13]. Concerning the phenomenological TBF (Urbana model), it contains a term that accounts for the so-called two-pion exchange contribution, with the creation of an intermediate excited  $\Delta$  state, and a phenomenological repulsive part (Ropler excitation) [14]. As shown in Ref.[4], using exactly the same values of parameters of the TBF for the two choices of NN two-body interaction indicated above, the difference between the corresponding EOS's, which are apparent in the case without TBF, are strongly reduced when TBF are introduced, not only around saturation, but for the whole density range. Hence, the overall effect of the same TBF on the EOS can be different according to the two-body force adopted, being less repulsive in the case when the two-body force is less attractive and pointing in the direction of making the EOS's closer to each other, see fig.1. This result is far from being trivial and it would be desirable to understand on physical grounds what is the interplay of two- and three-body forces in determining the nuclear EOS.

A different strategy is followed in Ref.[5]: TBF can be evaluated on the basis of a meson-exchange approach. Starting from two-body one-boson exchange (OBE) potentials, like the Bonn or Nijmegen potentials (see Ref.[5] and references therein), the meson exchange parameters of the TBF can be chosen completely consistent with the given NN potential, i.e. the same parameters

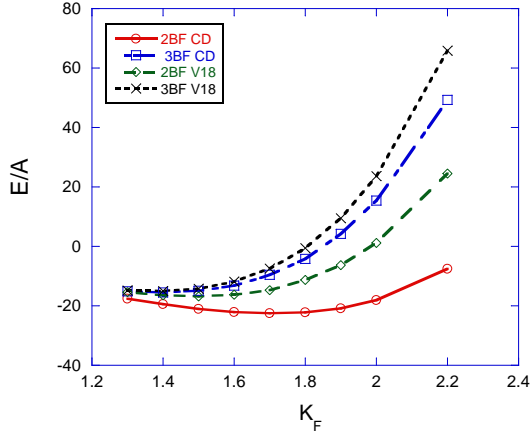


**Figure 1.** Equation of state of symmetric nuclear matter for the CD Bonn and the  $v_{18}$  two-body interactions and with the inclusion of three-body forces (TBF). The energy per particle  $E/A$  is in MeV and the Fermi momentum  $k_F$  is in  $fm^{-1}$ . Taken from Ref.[4]

are used in two and three-body forces. This kind of TBF involves the intermediate excitation of  $\Delta$ , Roper, and nucleon-antinucleon states by the exchange of  $\pi, \rho, \sigma$ , and  $\omega$  mesons in the TBF diagrams. However, one must be aware of the fact that some parameters are not given by the two-body force, in particular the ones related to  $\Delta$  and Roper excitation, and are evaluated according to recent prescriptions [5]. Contrary to what is done in Ref.[4], within this kind of approach, the nuclear matter saturation point is not fitted with the help of a phenomenological TBF, but it naturally arises from the full calculation, including two- and three-body forces and has to be checked against the experimental value. In fig.2 (middle panel), we report the EOS obtained

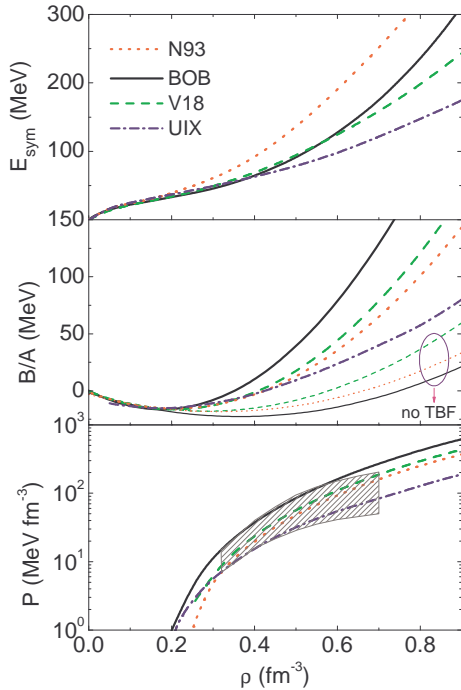


**Figure 2.** Symmetry energy (upper panel), binding energy per nucleon of symmetric nuclear matter (central panel), and pressure of symmetric matter (lower panel), employing different interactions. The shaded region indicates the constraints of Ref.[1]. Taken from Ref.[15].

with only two-body forces and with the full calculations, for different NN potentials. Also in this

case one can see that the effect of the TBF is more repulsive when the two-body force is more attractive. This is the kind of compensation discussed before. The result corresponding to the Urbana (phenomenological) TBF, coupled to the Argonne two-body interaction, is also shown on the figure (dot-dashed curve). Comparing dashed and dot-dashed lines, it appears that a very different behavior is obtained for the high density EOS and for the symmetry energy (middle panel) when using different TBF's, inspite of the fact that the saturation point is reasonably reproduced in all cases. One may notice, in particular, the rather stiff high density behavior obtained with the Bonn B (BOB) potential, for which the reproduction of the saturation point properties is excellent. The corresponding symmetry energy exhibits an interesting behavior, that is soft at low density and rather stiff at high density (see top panel).

From the results discussed here, one may conclude that the density behavior of the symmetric matter EOS and symmetry energy is still a rather open problem and it is thus very appealing to try to get hints from the phenomenology of nuclear reactions and nuclear astrophysics. We will review this kind of studies in the following, with a special emphasis on the information one can get on the density dependence of the symmetry energy.

### 3. Nuclear reactions and symmetry energy

Heavy ion reactions with neutron rich nuclei, from low up to relativistic energies, can be used to study the properties of the symmetry term of the nuclear interaction in a wide range of densities.

Nuclear reactions are modeled by solving transport equations based on mean field theories, with correlations included via hard nucleon-nucleon elastic and inelastic collisions and via stochastic forces, selfconsistently evaluated from the mean phase-space trajectory, see [16, 7]. Stochasticity is essential in order to get distributions as well as to allow for the growth of dynamical instabilities.

In the energy range up to a few hundred AMeV, the appropriate tool is the so-called Boltzmann-Langevin equation (BLE) [16]:

$$\frac{df}{dt} = \frac{\partial f}{\partial t} + \{f, H\} = I_{coll}[f] + \delta I[f], \quad (1)$$

where  $f(\mathbf{r}, \mathbf{p}, t)$  is the one-body distribution function, or Wigner transform of the one-body density,  $H(\mathbf{r}, \mathbf{p}, t)$  the mean field Hamiltonian,  $I_{coll}$  the two-body collision term incorporating the Fermi statistics of the particles, and  $\delta I[f]$  the fluctuating part of the collision integral. For higher beam energies, a covariant formulation of transport equations will be considered, see Section 5.2. Hence effective interactions and the nuclear matter EOS can be considered as ingredients of the transport codes and from the comparison with experimental data one can finally get some hints on nuclear matter properties.

We recall that the symmetry energy  $E_{sym}$  appears in the energy density  $\epsilon(\rho, \rho_3) \equiv \epsilon(\rho) + \rho E_{sym}(\rho_3/\rho)^2 + O(\rho_3/\rho)^4 + \dots$ , expressed in terms of total ( $\rho = \rho_p + \rho_n$ ) and isospin ( $\rho_3 = \rho_p - \rho_n$ ) densities.  $E_{sym}$  gets a kinetic contribution directly from basic Pauli correlations and a potential part,  $C(\rho)$ , from the highly controversial isospin dependence of the effective interactions:

$$\frac{E_{sym}}{A} = \frac{E_{sym}}{A}(kin) + \frac{E_{sym}}{A}(pot) \equiv \frac{\epsilon_F}{3} + \frac{C(\rho)}{2\rho_0}\rho \quad (2)$$

The sensitivity of the simulation results is tested against different choices of the density and momentum dependence of the isovector part of the Equation of State. In the non-relativistic frame, one can consider for the potential part of the symmetry energy,  $C(\rho)$ , two opposite density parametrizations (Iso-EOS) of the mean field [17, 7]: i)  $\frac{C(\rho)}{\rho_0} = 482 - 1638\rho$  ( $MeV fm^3$ ) for ‘‘Asysoft’’ EOS:  $E_{sym}/A(pot)$  has a weak density dependence close to the saturation, with an almost flat behavior below the saturation density  $\rho_0$  and even decreasing at suprasaturation;

ii) a constant coefficient,  $C = 32\text{MeV}$ , or a  $C(\rho)$  coefficient linearly increasing with density, for the ‘‘Asystiff’’ EOS choice: the interaction part of the symmetry term displays a faster decrease at lower densities and much stiffer above saturation, with respect to the Asysoft case, see fig.3. The isoscalar section of the EOS is the same in both cases, fixed requiring that the saturation properties of symmetric nuclear matter with a compressibility around  $220\text{MeV}$  are reproduced.

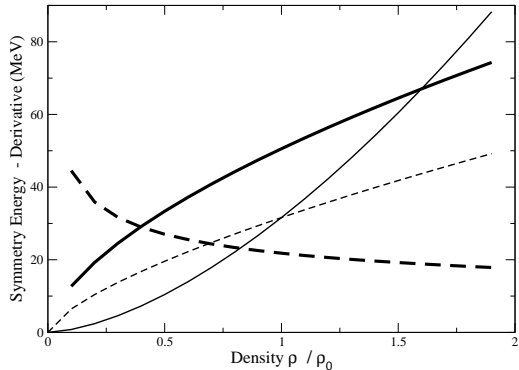


**Figure 3.** Two representative effective parameterizations of the symmetry energy (thin lines): asystiff (full line) and asysoft (dashed line). The tick lines show the corresponding derivatives.

The role of the isospin degree of freedom on the dynamics of a nuclear reaction can be discussed in a compact way by means of the chemical potentials for protons and neutrons as a function of density  $\rho$  and asymmetry  $I = (N - Z)/A$  [18]. The  $p/n$  currents can be expressed as

$$\mathbf{j}_{p/n} = D_{p/n}^\rho \nabla \rho - D_{p/n}^I \nabla I \quad (3)$$

with  $D_{p/n}^\rho$  the drift, and  $D_{p/n}^I$  the diffusion coefficients for transport, which are given explicitly in ref. [18]. Of interest for the study of isospin effects are the differences of currents between protons and neutrons which have a simple relation to the density dependence of the symmetry energy

$$\begin{aligned} D_n^\rho - D_p^\rho &\propto 4I \frac{\partial E_{sym}}{\partial \rho}, \\ D_n^I - D_p^I &\propto 4\rho E_{sym}. \end{aligned} \quad (4)$$

Thus the isospin transport due to density gradients, i.e. isospin migration, depends on the slope of the symmetry energy, or the symmetry pressure, while the transport due to isospin concentration gradients, i.e. isospin diffusion, depends on the absolute value of the symmetry energy. Hence transport phenomena in nuclear reactions are directly linked to the EOS properties.

#### 4. Symmetry energy at low density

At sub-saturation density, the symmetry energy of nuclear matter seems to be under control from the theoretical point of view since different microscopic many-body calculations agree among each other and TBF have a negligible effects [10, 19]. According to these calculations, the symmetry energy can be approximately described by  $E_{sym}/A = 31.3(\rho/\rho_0)^{0.6}$ . The existing data and analyses extracted from nuclear reactions [20, 21] seem to point to a behavior of the type  $E_{sym}/A \propto (\rho/\rho_0)^\gamma$ , with  $\gamma$  in the range  $0.6 - 1$ . Hence it is of great interest to pursue this investigation and devise new observables to test the behavior of the symmetry energy at low density.

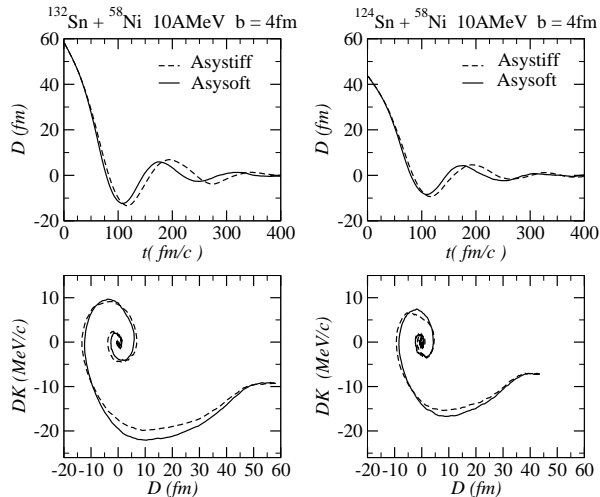


**Figure 4.** Dipole Dynamics at 10 AMeV,  $b = 4\text{fm}$  centrality. Left Panels: Exotic “132” system. Upper: Time evolution of dipole moment  $D(t)$  in real space; Lower: Dipole phase-space correlation (see text). Right Panels: same as before for the stable “124” system. Solid lines correspond to Asysoft EOS, the dashed to Asystiff EOS.

#### 4.1. The prompt dipole $\gamma$ -ray emission in dissipative collisions

The low-density behavior of the symmetry energy can be explored looking at dipole excitations in dissipative charge asymmetric reactions around 10 AMeV. The possibility of an entrance channel bremsstrahlung dipole radiation due to an initial different N/Z distribution was suggested at the beginning of the nineties [22]. After several experimental evidences, in fusion as well as in deep-inelastic reactions, [23, 24] and refs. therein, the process is now well understood and stimulating new perspectives are coming from the use of radioactive beams.

During the charge equilibration process taking place in the first stages of dissipative reactions between colliding ions with different N/Z ratios, a large amplitude dipole collective motion develops in the composite dinuclear system, the so-called Dynamical Dipole mode. This collective dipole gives rise to a prompt  $\gamma$ -ray emission which depends on the absolute value of the initial amplitude,  $D(t=0)$ , on the fusion/deep-inelastic dynamics and on the symmetry term, below saturation, that is acting as a restoring force. Indeed this oscillation develops in the low density interface between the two colliding ions (neck region).

A detailed description is obtained in mean field transport approaches [25]. One can follow the time evolution of the dipole moment in the  $r$ -space,  $D(t) = \frac{NZ}{A}(R_Z - R_N)$  and in  $p$ -space,  $DK(t) = (\frac{P_p}{Z} - \frac{P_n}{N})$ , being  $R_p$ ,  $P_p$  ( $R_n$ ,  $P_n$ ) the centers of mass in coordinate and momentum space for protons (neutrons). A nice “spiral-correlation” clearly denotes the collective nature of the mode, see fig.4. The “prompt” photon emission probability, with energy  $E_\gamma = \hbar\omega$ , can be estimated applying a bremsstrahlung approach to the dipole evolution given from the BLE approach [25]:

$$\frac{dP}{dE_\gamma} = \frac{2e^2}{3\pi\hbar c^3 E_\gamma} |D''(\omega)|^2, \quad (5)$$

where  $D''(\omega)$  is the Fourier transform of the dipole acceleration  $D''(t)$ . We remark that in this way it is possible to evaluate, in *absolute* values, the corresponding pre-equilibrium photon emission.

We must add a couple of comments of interest for the experimental selection of the Dynamical Dipole: i) The centroid is always shifted to lower energies (large deformation of the dinucleus);

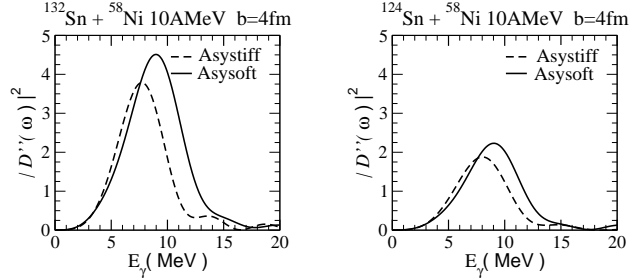


**Figure 5.** Left Panel, Exotic “132” system. Power spectra of the dipole acceleration at  $b = 4\text{fm}$  (in  $c^2$  units). Right Panel: Corresponding results for the stable “124” system. Solid lines correspond to Asysoft EOS, the dashed to Asystiff EOS.

ii) A clear angular anisotropy should be present since the prompt mode has a definite axis of oscillation (on the reaction plane) at variance with the statistical giant dipole resonance (*GDR*). These features have been observed in recent experiments [24].

The use of unstable neutron rich projectiles would largely increase the effect, due to the possibility of larger entrance channel asymmetries. This can be observed in figs.4,5, where the results of the reactions  $^{132}\text{Sn} + ^{58}\text{Ni}$  and  $^{124}\text{Sn} + ^{58}\text{Ni}$  are compared [26].

One can notice in fig.4 the large amplitude of the first oscillation for the “132” system, but also the delayed dynamics for the Asystiff EOS related to a weaker isovector restoring force. In fig.5 (Left Panel) we report the power spectrum,  $|D''(\omega)|^2$  in semicentral “132” reactions, for different *Iso* – *EOS* choices. The gamma multiplicity is simply related to it, see Eq.(5). The corresponding results for the stable “124” system are drawn in the Right Panel. As expected from the larger initial charge asymmetry, we clearly see an increase of the Prompt Dipole Emission for the exotic n-rich beam. Such entrance channel effect allows also for a better observation of the Iso-*EOS* dependence. We remind that in the Asystiff case we have a weaker restoring force for the dynamical dipole in the dilute “neck” region, where the symmetry energy is smaller, see fig.3. This is reflected in the lower value of the centroid,  $\omega_0$ , as well as in the reduced total yield, as shown in fig.5. The sensitivity of  $\omega_0$  to the stiffness of the symmetry energy is amplified by the increase of  $D(t_0)$  using exotic, more asymmetric beams.

The prompt dipole radiation angular distribution is the result of the interplay between the collective oscillation life-time and the dinuclear rotation. In this sense one expects also a sensitivity to the *Iso* – *EOS* of the anisotropy, in particular for high spin event selections [26].

#### 4.2. Isospin equilibration at the Fermi energies

In this energy range the doorway state mechanism of the Dynamical Dipole will disappear and so one can study a direct isospin transport in binary events. This process also involves the low density neck region and is sensitive to the low density behavior of  $E_{sym}$ , see Refs.[20],[27] and ref.s therein.

It is interesting to look at the asymmetries of the various parts of the reaction system in the exit channel: emitted particles, projectile-like (PLF) and target-like fragments (TLF), and in the case of ternary events, intermediate mass fragments (IMF). In particular, one can study the so-called Imbalance Ratio, which is defined as

$$R_{P,T}^x = \frac{2(x^M - x^{eq})}{(x^H - x^L)}, \quad (6)$$

with  $x^{eq} = \frac{1}{2}(x^H + x^L)$ . Here,  $x$  is an isospin sensitive quantity that has to be investigated with respect to equilibration. We consider primarily the asymmetry  $\beta = I = (N - Z)/A$ , but

also other quantities, such as isoscaling coefficients, ratios of production of light fragments, etc, can be of interest [8]. The indices  $H$  and  $L$  refer to the symmetric reaction between the heavy ( $n$ -rich) and the light ( $n$ -poor) systems, while  $M$  refers to the mixed reaction.  $P, T$  denote the rapidity region, in which this quantity is measured, in particular the PLF and TLF rapidity regions. Clearly, this ratio is  $\pm 1$  in the projectile and target regions, respectively, for complete transparency, and oppositely for complete rebound, while it is zero for complete equilibration.

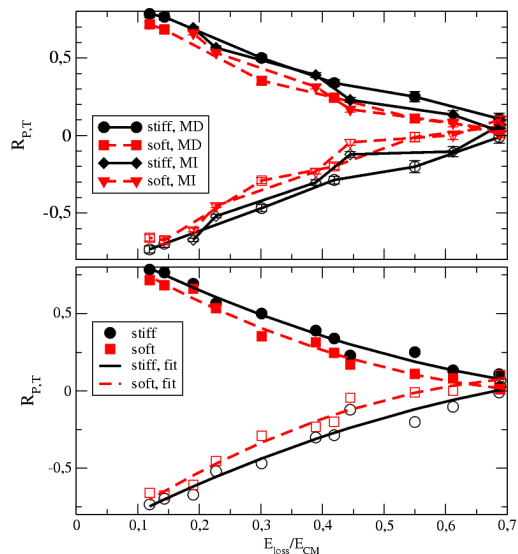


**Figure 6.** Imbalance ratios as a function of relative energy loss. Upper: Separately for stiff (solid) and soft (dashed) iso-EOS, and for two parameterizations of the isoscalar part of the interaction: MD (circles and squares) and MI (diamonds and triangles), in the projectile region (full symbols) and the target region (open symbols). Lower: Quadratic fit to all points for the stiff (solid), resp. soft (dashed) iso-EOS.

In a simple model one can show that the imbalance ratio mainly depends on two quantities: the strength of the symmetry energy and the interaction time between the two reaction partners. Let us take, for instance, the asymmetry  $\beta$  of the PLF (or TLF) as the quantity  $x$ . At a first order approximation, in the mixed reaction this quantity relaxes towards its complete equilibration value,  $\beta_{eq} = (\beta_H + \beta_L)/2$ , as

$$\beta_{P,T}^M = \beta^{eq} + (\beta^{H,L} - \beta^{eq}) e^{-t/\tau}, \quad (7)$$

where  $t$  is the time elapsed while the reaction partners stay in contact (interaction time) and the damping  $\tau$  is mainly connected to the strength of the symmetry energy [27]. Inserting this expression into Eq.(6), one obtains  $R_{P,T}^\beta = \pm e^{-t/\tau}$  for the PLF and TLF regions, respectively. Hence the imbalance ratio can be considered as a good observable to trace back the strength of the symmetry energy from the reaction dynamics provided a suitable selection of the interaction time is performed.

The centrality dependence of the Imbalance Ratio, for (Sn,Sn) collisions at 35 and 50 AMeV, has been investigated in experiments as well as in theory [18, 20]. We report here a new analysis which appears experimentally more selective [27]. Longer interaction times should be correlated to a larger dissipation. It is then natural to look at the correlation between the imbalance ratio and the total kinetic energy loss. In this way one can also better disentangle dynamical effects of the isoscalar and isovector part of the EOS, see [27].

It is seen in fig.6 (top) that the curves for the *Asysoft* EOS (dashed) are generally lower in the projectile region (and oppositely for the target region), i.e. show more equilibration, than those for the *Asystiff* EOS, due to the higher value of the symmetry energy at low density. To emphasize this trend, all the values for the stiff (circles) and the soft (squares)



iso-EOS, corresponding to different impact parameters, beam energies and also to two possible parameterizations of the isoscalar part of the nuclear interaction (MD and MI) are collected together in the bottom part of the figure. One can see that all the points essentially follow a given line, depending only on the symmetry energy parameterization adopted. It is seen, that there is a systematic effect of the symmetry energy of the order of about 20 percent, which should be measurable. The correlation suggested in fig.6 should represent a general feature of isospin diffusion, and it would be of great interest to verify it experimentally.

#### 4.3. Dipole emission in peripheral collisions at relativistic energies

Here we briefly review results obtained with more macroscopic models on dipole excitation in peripheral collisions, such as  $^{40}\text{Ca} + ^{24}\text{O}$  at 500 AMeV. In Ref.[28] a relativistic treatment is elaborated, to derive the equations of motion of (projectile and target) neutron and proton centroids, under the action of the restoring isovector nuclear force, taking into account in the excitation of the dipole oscillations, apart from Coulomb effects, also the contribution of the nuclear potential, treated with a Wood-Saxon potential well. It is observed that mean-field effects give a strong contribution to the excitation of the dipole oscillation, that is connected to the neutron skin of the target nucleus, leading to a different attraction between the target protons or neutrons and the projectile nucleons. The actual cross section for one- or two-phonon excitations is then evaluated according to the expression  $\sigma_\alpha = 2\pi \int_0^\infty P_\alpha(b)T(b)bdb$ , where  $P_\alpha(b)$  is the probability, at the impact parameter  $b$ , for a given reaction channel  $\alpha$ . This is related to the number of phonons,  $N_{ph} = E_\infty/(\hbar\omega)$  excited by the driving force, being  $E_\infty$  the energy associated with the dipole oscillations at asymptotic distance.  $T(b)$  are attenuation factors that take into account the depopulation of the reaction channels due to couplings not explicitly included in the truncated working space.

Comparing the obtained cross sections to experimental data, from these studies one can get information on the neutron skin structure of neutron-rich systems that, in turn, depends on the low density behavior of the symmetry energy.

#### 4.4. Isospin distillation in central collisions

In central collisions at 30-50 AMeV, where the full disassembly of the system into many fragments is observed, one can study specifically properties of liquid-gas phase transitions occurring in asymmetric matter [29, 16, 7, 9, 30]. For instance, in neutron-rich matter, phase co-existence leads to a different asymmetry in the liquid and gaseous phase: fragments (liquid) appear more symmetric with respect to the initial matter, while light particles (gas) are more neutron-rich. The amplitude of this "distillation" effect, that is connected to the presence of density gradients in the system, depends on specific properties of the isovector part of the nuclear interaction, namely on the value and the derivative of the symmetry energy at low density (see also the discussion in Section 3). Indeed, since the symmetry energy increases with density, it is energetically more convenient for asymmetric systems to transfer the neutron excess to the gas phase, while fragments (liquid phase) become more symmetric. These features can be easily evidenced by studying fragment formation in unstable asymmetric nuclear matter inside a box. In fig.7 (left) the N/Z of the domains formed inside the box is reported as a function of the density, for systems with two initial charge asymmetry values and for two Iso-EOS employed. The variance of the (N-Z) difference inside the density domains is displayed on the right part of the figure, as a function of the volume of the domain considered. One can see that, both the average N/Z and the isovector variance decrease as the density increases, leading to a more symmetric and less fluctuating liquid phase. However, fluctuations are rather large in the Asysoft case (circles and triangles) [31].

The investigation of isospin distillation is interesting in a more general context: In heavy ion collisions the dilute phase appears during the expansion of the interacting matter. Thus we

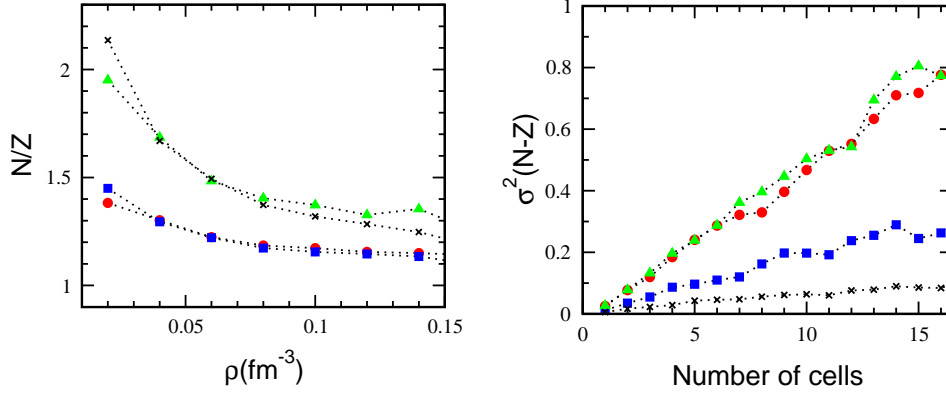


**Figure 7.** Left Panel: Correlation between the  $N/Z$  and the density of the domains, obtained with the two asy-EOS in the decomposition of unstable nuclear matter, with asymmetry  $\beta = 0.1$  (squares and circles) and  $\beta = 0.2$  (triangles and stars). Right: Variance of the  $(N-Z)$  content of the density domains as a function of their volume [31].

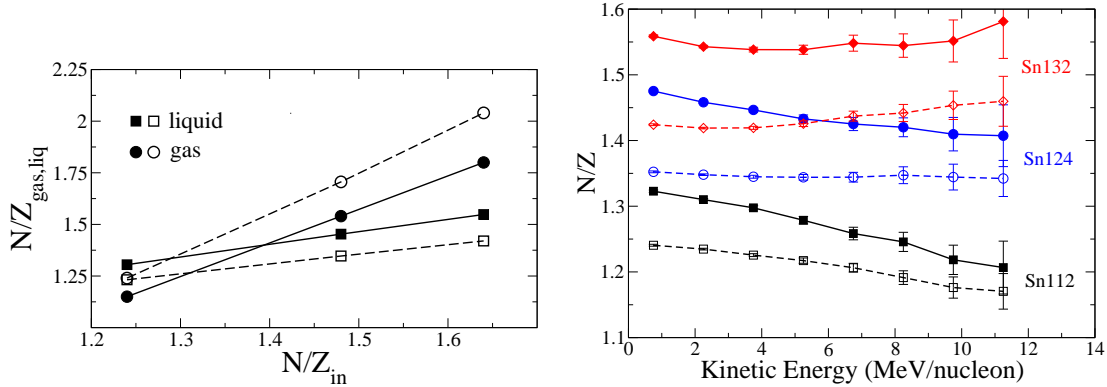


**Figure 8.** Left Panel. The  $N/Z$  of the liquid (squares) and of the gas (circles) phase is displayed as a function of the system initial  $N/Z$ . Full lines and symbols refer to the asystiff parameterization. Dashed lines and open symbols are for asysoft. Right Panel. The fragment  $N/Z$  as a function of the kinetic energy. Full lines: Asystiff; Dashed lines: Asysoft.

study effects of the coupling of expansion, fragmentation and distillation in a two-component (neutron-proton) system [32]. Let us focus now on actual collisions, considering symmetric reactions between systems having three different initial asymmetry:  $^{112}\text{Sn} + ^{112}\text{Sn}$ ,  $^{124}\text{Sn} + ^{124}\text{Sn}$ ,  $^{132}\text{Sn} + ^{132}\text{Sn}$ , with  $(N/Z)_{\text{in}} = 1.24, 1.48, 1.64$ , respectively. The considered beam energy is 50 A MeV. The average  $N/Z$  of emitted nucleons (gas phase) and IMF's is presented in fig.8 (Left Panel) as a function of the initial  $(N/Z)_{\text{in}}$  of the three colliding systems. One observes a clear Isospin-Distillation effect, i.e. the gas phase (circles) is more neutron-rich than the IMF's (squares). This is particularly evident in the Asysoft case due to the larger value of the symmetry energy and of its derivative at low density [7].

Fragmentation originates from the break-up of a composite source that expands with a given velocity field. Since neutrons and protons experience different forces, one may expect a different radial flow for the two species. In this case, the  $N/Z$  composition of the source would not be uniform, but would depend on the radial distance from the center or mass or, equivalently, on

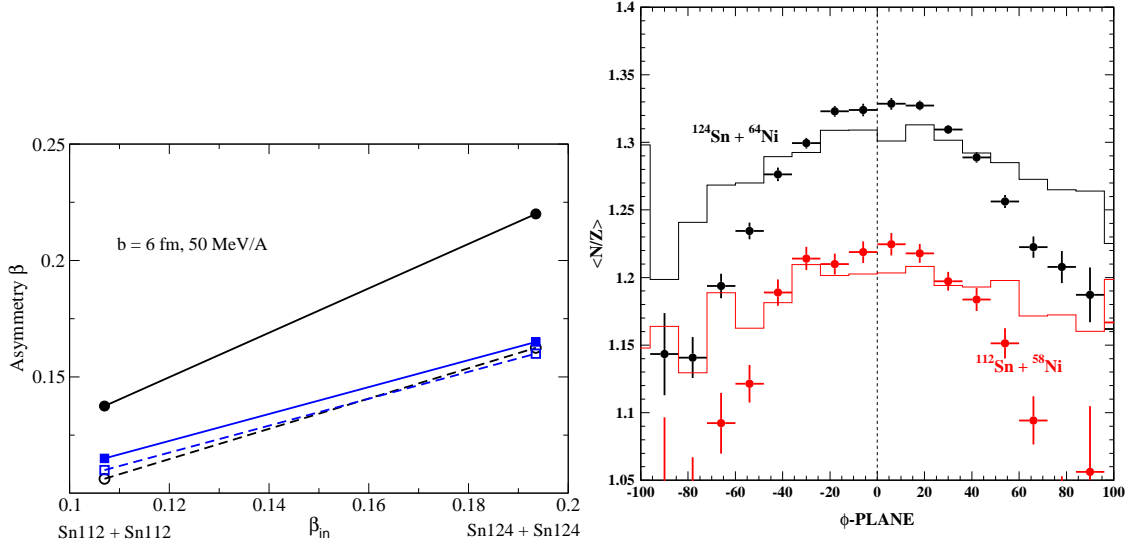


**Figure 9.** Left: Asymmetry of IMF's (circles) and PLF-TLF (squares), as a function of the system initial asymmetry, for two iso-EOS choices: Asystiff (full lines) and Asysoft (dashed lines). Right: Exp. results on correlation between  $N/Z$  of IMF and *alignment* in ternary events of the  $^{124}\text{Sn} + ^{64}\text{Ni}$  and  $^{112}\text{Sn} + ^{58}\text{Ni}$  reactions at 35 AMeV. Points correspond to fast formed IMFs; histograms to all IMFs at mid-rapidity (including statistical emissions). From Ref.[33]

the local velocity. It has been recently proposed that this trend should then be reflected in a clear correlation between isospin content and kinetic energy of the formed IMF's [32].

This observable is plotted in fig.8 (Right Panel) for the three reactions. The behaviour observed is rather sensitive to the Iso-EOS. For the proton-rich system, the  $N/Z$  decreases with the fragment kinetic energy, especially in the Asystiff case (left), where the symmetry energy is relatively small at low density. In this case, the Coulomb repulsion pushes the protons towards the surface of the system. Hence, more symmetric fragments acquire larger velocity. The decreasing trend is less pronounced in the Asysoft case (right) because Coulomb effects on protons are counterbalanced by the larger attraction of the symmetry potential at low density. In systems with higher initial asymmetry, the decreasing trend is inverted, due to the larger neutron repulsion in neutron-rich systems. This analysis reveals the existence of significant, EOS-dependent correlations between the  $N/Z$  and the kinetic energy of IMF's produced in central collisions. This appears as a promising experimental observable to be investigated, though fragment secondary effects are expected to reduce the sensitivity to the iso-EOS [32].

#### 4.5. Isospin dynamics in neck fragmentation at Fermi energies

It is now quite well established that the largest part of the reaction cross section for dissipative collisions at Fermi energies goes through the *Neck Fragmentation* channel, with IMFs directly produced in the interacting zone in semiperipheral collisions on very short time scales [34]. It is possible to predict interesting isospin transport effects for this fragmentation mechanism since clusters are formed still in a dilute asymmetric matter but always in contact with the regions of the projectile-like and target-like remnants almost at normal densities. As discussed in Sect.3, in presence of density gradients the isospin transport is mainly ruled by drift coefficients and so we expect a larger neutron flow to the neck clusters for a stiffer symmetry energy around saturation [7]. This is shown in fig.9 (left), where the asymmetry of the neck region of charge

asymmetric reactions is plotted for two Iso-EOS choices.

A very nice new analysis has been performed on the  $Sn + Ni$  data at 35  $AMeV$  by the Chimera Collab.[33], see fig.9 right panel. A strong correlation between neutron enrichment and fragment alignment (when the short emission time selection is enforced) is seen, that points to a stiff behavior of the symmetry energy, for which a large neutron enrichment of neck fragments is seen (left). This represents a clear evidence in favor of a relatively large slope (symmetry pressure) around saturation. We note a recent confirmation from structure data, i.e. from monopole resonances in Sn-isotopes [35].

## 5. Iso-EOS at supra-saturation density

### 5.1. Effective mass splitting and collective flows

The problem of Momentum Dependence in the Isovector channel ( $Iso - MD$ ) of the nuclear interaction is still very controversial and it would be extremely important to get more definite experimental information, see the recent refs. [36, 37]. Exotic Beams at intermediate energies (100-500  $AMeV$ ) are of interest in order to have high momentum particles and to test regions of high baryon (isoscalar) and isospin (isovector) density during the reaction dynamics. Transport codes are usually implemented with different  $(n, p)$  momentum dependences, see [37, 36]. This allows one to follow the dynamical effect of opposite n/p effective mass ( $m^*$ ) splitting while keeping the same density dependence of the symmetry energy [27].

For central collisions in the interacting zone baryon densities about  $1.7 - 1.8\rho_0$  can be reached in a transient time of the order of 15-20 fm/c. The system is quickly expanding and the Freeze-Out time is around 50fm/c. Here it is very interesting to study again the collective response of the system. Collective flows are very good candidates since they are expected to be rather sensitive to the momentum dependence of the mean field, see [38, 7]. The transverse flow,  $V_1(y, p_t) = \langle \frac{p_x}{p_t} \rangle$ , provides information on the anisotropy of nucleon emission on the reaction plane. Very important for the reaction dynamics is the elliptic flow,  $V_2(y, p_t) = \langle \frac{p_x^2 - p_y^2}{p_t^2} \rangle$ . The sign of  $V_2$  indicates the azimuthal anisotropy of emission: on the reaction plane ( $V_2 > 0$ ) or out-of-plane (*squeeze-out*,  $V_2 < 0$ ) [38]. The  $Iso - MD$  of the fields can be tested just evaluating the difference of neutron/proton transverse and elliptic flows  $V_{1,2}^{(n-p)}(y, p_t) \equiv V_{1,2}^n(y, p_t) - V_{1,2}^p(y, p_t)$  at various rapidities and transverse momenta in semicentral ( $b/b_{max} = 0.5$ ) collisions, such as  $^{197}Au + ^{197}Au$  at 400  $AMeV$ . For the nucleon elliptic flows the mass splitting effect is evident at all rapidities, and nicely increasing at larger rapidities and transverse momenta, with more neutron flow when  $m_n^* < m_p^*$ . From fig.10 it is clear how at, mid-rapidity, the mass

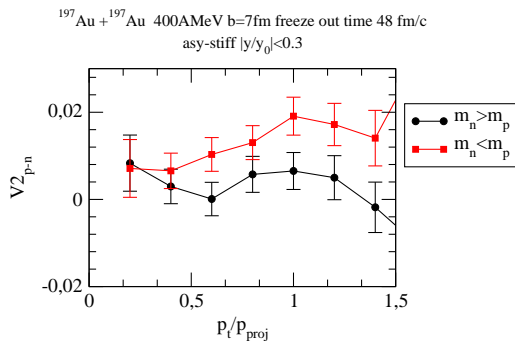


**Figure 10.** Transverse momentum dependence of the difference between proton and neutron  $V_2$  flows, at mid-rapidity, in a semi-central reaction  $Au+Au$  at 400 $AMeV$ . Taken from Refs.[39],[40].

splitting effects are more evident for higher transverse momentum selections, i.e. for high density sources. In particular the elliptic flow difference becomes negative when  $m_n^* < m_p^*$ , revealing a faster neutron emission and so more neutron squeeze out (more spectator shadowing). In correspondance the proton flow is more negative (more proton squeeze out) when  $m_n^* > m_p^*$ .

Due to the difficulties in measuring neutrons, one could investigate the difference between light isobar flows, like  ${}^3H$  vs.  ${}^3He$ . We still expect to see effective mass splitting effects.

### 5.2. Meson production in relativistic heavy ion collisions

The phenomenology of isospin effects on heavy ion reactions at relativistic energies (few  $AGeV$  range) is extremely rich and can allow a “direct” study of the covariant structure of the isovector interaction in a high density hadron medium. In this energy range, one has to work within a relativistic transport frame, beyond the cascade picture, consistently derived from effective Lagrangians, where isospin effects are accounted for in the mean field and collision terms. Heavy ion collisions are described solving the covariant transport equation of the Boltzmann type (RBUU) [41], and applying a Monte-Carlo procedure for the hard hadron collisions. The collision term includes elastic and inelastic processes involving the production/absorption of the  $\Delta(1232MeV)$  and  $N^*(1440MeV)$  resonances as well as their decays into pion channels [42].

The effective Lagrangian approach to the hadron interacting system can be extended to the isospin degree of freedom: within the same frame equilibrium properties ( $EOS$ , [43]) and transport dynamics can be consistently derived. Within a covariant picture of the nuclear mean field, for the description of the symmetry energy at saturation (a) only the Lorentz vector  $\rho$  mesonic field, and (b) both, the vector  $\rho$  (repulsive) and scalar  $\delta$  (attractive) effective fields are included. In the latter case a rather intuitive form of the symmetry energy can be obtained [7]

$$E_{sym} = \frac{1}{6} \frac{k_F^2}{E_F} + \frac{1}{2} \left[ f_\rho - f_\delta \left( \frac{m^*}{E_F} \right)^2 \right] \rho_B. \quad (8)$$

The competition between scalar and vector fields leads to a stiffer symmetry term at high density [7].

To discuss meson production, the starting point is a simple phenomenological version of the Non-Linear (with respect to the iso-scalar, Lorentz scalar  $\sigma$  field) effective nucleon-boson field theory, the Quantum-Hadro-Dynamics [43]. According to this picture the presence of the hadronic medium leads to effective masses and momenta  $M^* = M + \Sigma_s$ ,  $k^{*\mu} = k^\mu - \Sigma^\mu$ , with  $\Sigma_s$ ,  $\Sigma^\mu$  scalar and vector self-energies. For asymmetric matter the self-energies are different for protons and neutrons, depending on the isovector meson contributions. The corresponding models are named  $NL\rho$  and  $NL\rho\delta$ , respectively, and just  $NL$  for the case without isovector interactions. For the more general  $NL\rho\delta$  case the self-energies of protons and neutrons read:

$$\begin{aligned} \Sigma_s(p, n) &= -f_\sigma \sigma(\rho_s) \pm f_\delta \rho_{s3}, \\ \Sigma^\mu(p, n) &= f_\omega j^\mu \mp f_\rho j_3^\mu, \end{aligned} \quad (9)$$

(upper signs for neutrons), where  $\rho_s = \rho_{sp} + \rho_{sn}$ ,  $j^\alpha = j_p^\alpha + j_n^\alpha$ ,  $\rho_{s3} = \rho_{sp} - \rho_{sn}$ ,  $j_3^\alpha = j_p^\alpha - j_n^\alpha$  are the total and isospin scalar densities and currents and  $f_{\sigma,\omega,\rho,\delta}$  are the coupling constants of the various mesonic fields.  $\sigma(\rho_s)$  is the solution of the non linear equation for the  $\sigma$  field [7]. From the form of the scalar self-energies we note that in n-rich environment the neutron effective masses are definitely below the proton ones.

Kaon production has been proven to be a reliable observable for the high density  $EOS$  in the isoscalar sector [44]. Here we show that the  $K^{0,+}$  production (in particular the  $K^0/K^+$  yield ratio) can be also used to probe the isovector part of the  $EOS$  [42]. Pion and kaon production are analyzed in central  ${}^{197}Au + {}^{197}Au$  collisions in the  $0.8 - 1.8 AGeV$  beam energy range [42].

When isovector fields are included the symmetry potential energy in neutron-rich matter is repulsive for neutrons and attractive for protons. In a heavy ion collision this leads to a fast, pre-equilibrium, emission of neutrons. Such a *mean field* mechanism, often referred to as isospin fractionation [7], is responsible for a reduction of the neutron to proton ratio during the high

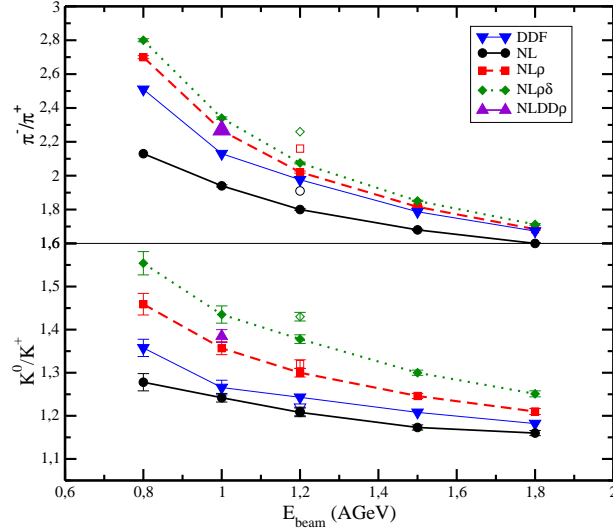


**Figure 11.**  $\pi^-/\pi^+$  (top) and  $K^0/K^+$  (bottom) ratios as a function of the incident energy for central Au + Au collisions, for several parameterizations of the isovector nuclear interaction. The open symbols at 1.2 AGeV show the corresponding results for a  $^{132}\text{Sn} + ^{124}\text{Sn}$  collision, more neutron rich.

density phase, with direct consequences on particle production in inelastic  $NN$  collisions. On the other hand, the self-energy contributions, Eqs.9, will influence the particle production at the level of thresholds as well as of the phase space available in the final channel. As a matter of fact, the threshold effect is dominant and consequently the results are nicely sensitive to the covariant structure of the isovector fields, see fig.11. The beam energy dependence of the  $\pi^-/\pi^+$  (top) and  $K^0/K^+$  (bottom) ratios is shown on the figure. At each beam energy we see an increase of the  $\pi^-/\pi^+$  and  $K^0/K^+$  yield ratios with the models  $NL \rightarrow NL\rho \rightarrow NL\rho\delta$ . The effect is larger for the  $K^0/K^+$  compared to the  $\pi^-/\pi^+$  ratio. This is due to the subthreshold production and to the fact that the isospin effect enters twice in the two-step production of kaons, see [42]. Interestingly the Iso- $EOS$  effect for pions is increasing at lower energies, when approaching the production threshold.

## 6. Hints from neutron stars

Neutron stars appear as natural astrophysical laboratories to study the behavior of the EOS at high density. In particular, the structure and composition of neutron stars is affected by the density dependence of the symmetry energy. Neutron stars are long-lived systems in  $\beta$  equilibrium, hence in rather different conditions with respect to the transient systems that are formed in nuclear reactions. The concept of EOS is very appropriate for these objects, but experimental observations of their properties are more difficult.

It is generally believed that a neutron star (NS) is formed as a result of the gravitational collapse of a massive star in a type-II supernova. Hence a protoneutron star (PNS) appears, a very hot and lepton-rich object, where neutrinos are temporarily trapped. The following evolution of the PNS is dominated by neutrino diffusion, which eventually results in cooling. The star stabilizes at practically zero temperature, and no trapped neutrinos are left.

The dynamical transformation of a PNS into a NS could be strongly influenced by a phase transition in the central region of the star. In fact, the central particle density of a massive PNS may reach values larger than  $1/fm^3$ . In this density range the nucleon cores start to touch each other, and it is likely that quark degrees of freedom will play a role.

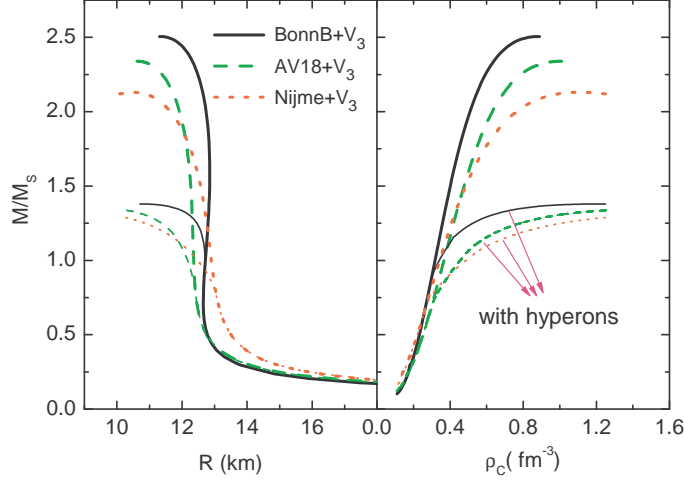


**Figure 12.** Mass-radius (left panel) and mass-central density (right panel) relations of neutron stars evaluated with different nucleonic EOS. Taken from Ref.[15].

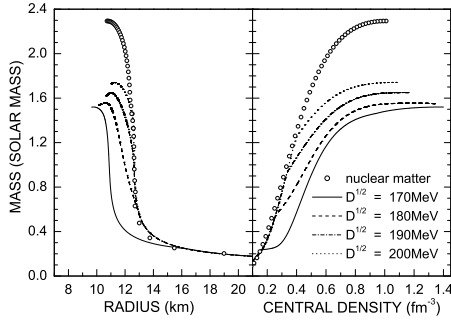


**Figure 13.** Mass-radius (left panel) and mass-central density (right panel) relations of hybrid stars for four values of the confinement parameter  $D$ . The nucleonic EOS is the one corresponding to the BOB interaction, see fig.2. Taken from Ref.[45].

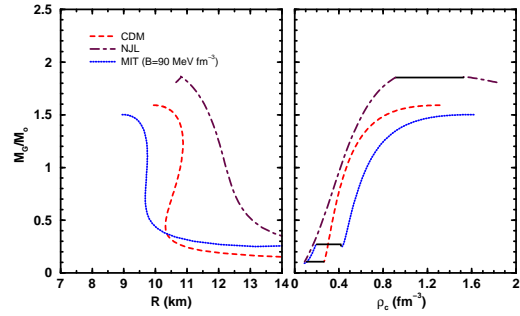


**Figure 14.** Mass-radius (left panel) and mass-central density (right panel) relations of hybrid stars, corresponding to three different models of the quark phase. The hadronic EOS includes hyperons. Adapted from Refs.[46],[48].

For stars in which the strongly interacting particles are only baryons, the composition at given baryon density  $\rho_B$  is determined by the requirements of  $\beta$  equilibrium and charge neutrality, involving nucleons, hyperons, leptons (electrons, muons) and neutrinos [45, 46]. These conditions fix, at the density  $\rho_B$ , and for given muon and electron numbers, the relative densities of all species. From the knowledge of these densities, using the Fermi-gas model for leptons, (non-interacting) hyperons and for neutrinos and the usual thermodynamical relation  $P = \rho^2 \frac{\partial(f/\rho)}{\partial \rho}$  (being  $f$  the free-energy density) for neutrons and protons, one finally obtains the EOS of the matter that composes the star, i.e. the pressure corresponding to  $\rho_B$ ,  $P(\rho_B)$ . The result clearly depends on the nucleonic EOS adopted, usually taken from microscopic calculations, see Section 2. Nucleon-hyperon interactions can also be included [46, 15].

To investigate the possible phase transition to quark matter in neutron stars, it is essential to know also the EOS of the quark matter. One usually deals with ordinary strange quark matter (SQM) in  $\beta$  equilibrium. The special problem in studying the EOS of ordinary quark matter is to treat quark confinement in a proper way. The conventional standard approach is to add an extra constant term to the quark energy, the bag constant  $B$  (MIT bag model), that leads to a negative contribution to the pressure, to confine quarks in a finite volume [46]. Alternatively, in Ref.[45] the quark confinement is treated using the chirally dependent quark mass scaling, where the quark mass scales with density. From the weak-equilibrium conditions of SQM, for given baryon and charge densities, it is possible to get the the relative densities of quarks (u,d,s) and electrons and finally derive the EOS of the quark matter [45].

The possible co-existence between quark and hadronic matter is studied imposing the Gibbs conditions [47]. Requiring the equality of the chemical potentials in the two phases, only two chemical potentials remain independent, such as  $(\mu_n, \mu_p)$  for instance. Their corresponding values as well as the quark fraction, are determined by imposing to have the same pressure in the two phases at the given total  $\rho_B$  and electric charge.

Calculations show that the transition from the hadron to the mixed phase occurs at a density a bit less than  $0.15 \text{ fm}^{-3}$ , close to the saturation density. Of course, this is not the case in terrestrial laboratories, since the nuclear matter so far realized in exotic nuclei or heavy ion collisions is much less neutron-rich than neutron stars. However, the transition to the pure quark phase occurs at much higher density, of the order of  $0.6 \text{ fm}^{-3}$ . The transition density depends on the MIT bag parameter or, in the case of the density dependent quark masses, on the parameter usually named  $D$  [45]. One can note that, increasing the bag parameter  $B$ , the pressure associated with the quark phase decreases and the transition starts at higher density. It is worth mentioning that the asymmetry of the quark phase is higher than the asymmetry of the co-existing hadronic phase.

With the EOS which has the mixed and/or quark phases at hand, the structure of hybrid stars can be studied by solving the Tolmann-Oppenheimer-Volkoff (TOV) equation:

$$\frac{dP}{dr} = -\frac{GmE}{r^2} \frac{(1 + P/E)(1 + 4\pi r^3 P/m)}{1 - 2Gm/r}, \quad (10)$$

where  $G$  is the gravitational constant,  $r$  is the distance from the center of the star,  $E = E(r)$  and  $P = P(r)$  are the energy density and pressure at the radius  $r$ , respectively. The EOS  $P = P(E)$  is essentially the input of the equation. The subsidiary condition is:

$$dm/dr = 4\pi r^2 E, \quad (11)$$

where  $m(r)$  denotes the gravitational mass of the star. Starting with a central mass density  $E_C$ , Eq.(10) is integrated out until the pressure on the surface equals the one corresponding to the density of iron. This gives the stellar radius  $R$  and the gravitational mass  $M_G$ . In particular, one can investigate the maximum radius of stable stars.

As one can see from fig.12, a remarkable reduction of the large range of the maximum mass obtained with the nucleonic EOS's ( $1.8\text{-}2.5 M_\odot$ ) to the nearly unique value of  $1.3\text{-}1.4 M_\odot$  is observed when only hyperons are included in the calculation of the nuclear EOS, i.e. excluding the possible transition to the quark matter, but implementing the nucleon-hyperon interaction in the EOS. The hyperons provide a self-regulating softening effect on the EOS: The stiffer the original nucleonic EOS, the more it is softened by the earlier appearance at higher concentration of hyperons. Due to the softening of the EOS, the maximum stellar mass decreases.

In any case, the maximum masses of hadronic (hyperonic) neutron stars are much too low in order to cover all present observational values. Within the present descriptions, the introduction of nonhadronic "quark" matter is thus necessary and heavier neutron stars can only be hybrid



stars. Some calculations including the possibility of a transition (or co-existence) to the quark phase are shown in figs.13,14. Results obtained with different possibilities to model the quark phase and different nucleonic EOS are presented. With the inclusion of quarks, one obtains a maximum mass in the range 1.4-1.8  $M_{\odot}$ , that depends on the model considered, but is closer to the experimental observations. The largest value is obtained adopting the Nambu-Jona Lasinio (NJL) model for the quark phase [48]. Indeed, in this case, the co-existence with the quark phase starts at rather high density and no transition at all is observed if hyperons are also included. Moreover, the onset of the pure quark phase at the center of the PNS as the mass increases marks an instability of the star, i.e. the PNS collapses to a black hole at the transition point since the quark EOS is unable to sustain the increasing central pressure due to gravity.

From the body of these calculations, one can conclude that limiting masses for PNS smaller than 2 solar masses are generally confirmed in all models .

All that shows clearly the great relevance of observations on NS to our knowledge of the high density nuclear EOS. The astrophysical observations could be able to rule out definite EOS or put constraints on them. However, the results discussed above indicate a larger sensitivity to the model adopted for the quark phase than to the nucleonic EOS.

## 7. On the transition to a mixed hadron-quark phase in HIC at relativistic energies

The possibility of the transition to a mixed hadron-quark phase, at high baryon and isospin density, has been suggested also for the dense and hot matter that is formed in HIC of charge asymmetric systems at relativistic energies, such as for instance  $Au + Au$  or  $^{238}U + ^{238}U$  (average proton fraction  $Z/A = 0.39$ ) at 1  $AGeV$ .

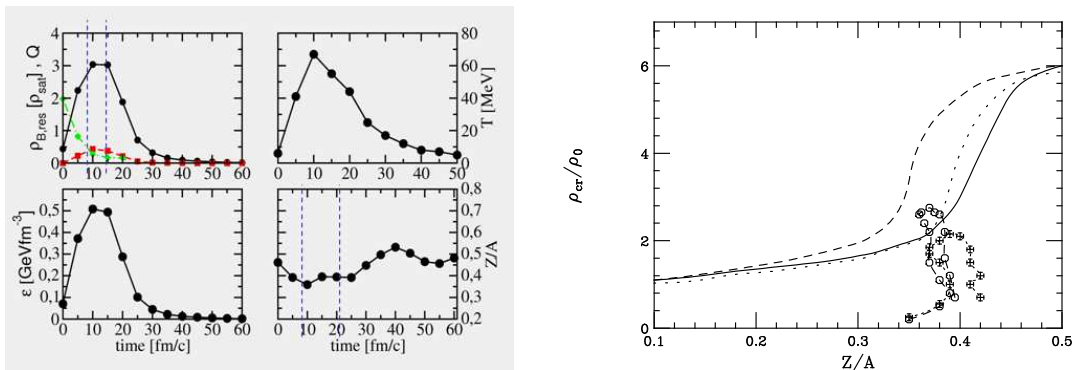


**Figure 15.** Left: Time evolution of density, temperature, energy density and  $Z/A$  content reached in a central region of the reaction  $Au + Au$  at 1  $AGeV$ , as obtained in RBUU calculations. Right: Variation of the transition density with proton fraction for various hadronic EOS parameterizations. Dotted line: *GM3 RMF*-model [49]; dashed line: *NL $\rho$*  ; solid line: *NL $\rho\delta$*  . For the quark EOS: *MIT* bag model with  $B^{1/4}=150$   $MeV$ . The points represent the path followed in the interaction zone during a semi-central  $^{132}Sn + ^{132}Sn$  collision at 1  $AGeV$  (circles) and at 300  $AMeV$  (crosses). From Ref.[50].

In fig. 15 (left) we discuss the evolution of temperature, baryon density, energy density and  $Z/A$  in a space cell located in the c.m. of the system. We note that a rather exotic nuclear matter is formed in a transient time of the order of 10  $fm/c$ , with baryon density around  $3-4\rho_0$ , temperature 50 – 60  $MeV$ , energy density 500  $MeV fm^{-3}$  and proton fraction between 0.35 and 0.40, likely inside the estimated mixed phase region.

In fact the transition densities are largely isospin dependent and, as seen in the previous Section in the case of neutron stars, reach rather low values in very asymmetric matter.

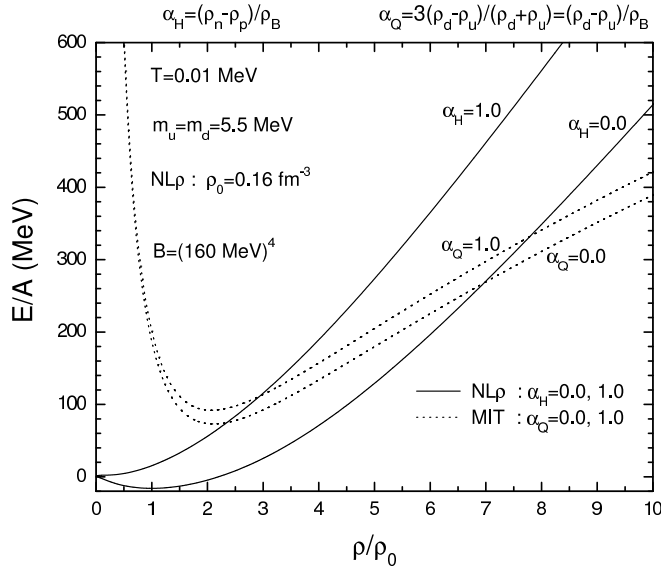


**Figure 16.** *EOS* of Symmetric/Neutron Matter: Hadron ( $NL\rho$ ), solid lines, vs. Quark (MIT-Bag), dashed lines.  $\alpha_{H,Q}$  represent the isospin asymmetry parameters respectively of the hadron, quark matter:  $\alpha_{H,Q} = 0$ , Symmetric Matter;  $\alpha_{H,Q} = 1$ , Neutron Matter. Taken from Ref.[40].

In the hadronic phase the charge chemical potential is given by  $\mu_3 = 2E_{sym}(\rho_B)\frac{\rho_3}{\rho_B}$ . Thus, we expect critical densities rather sensitive to the isovector channel in the hadronic *EOS*.

In fig. 15 (right) we show the crossing density  $\rho_{cr}$  separating nuclear matter from the quark-nucleon mixed phase, as a function of the proton fraction  $Z/A$ , for different parameterizations of  $E_{sym}$ , see Section 5.2. The MIT bag model is adopted for the quark phase. We can see the effect of the  $\delta$ -coupling towards an *earlier* crossing due to the larger symmetry repulsion at high baryon densities. In the same figure the paths in the  $(\rho, Z/A)$  plane followed in the c.m. region during the collision of the n-rich  $^{132}\text{Sn}+^{132}\text{Sn}$  system, at different beam energies, are also reported. One can see that already at 300  $A\text{MeV}$  the systems may be on the border of the mixed phase, and well inside it at 1  $A\text{GeV}$  [50].

As a signature of co-existence with quark matter in HIC, one can expect a *neutron trapping* effect, supported by statistical fluctuations as well as by a symmetry energy difference in the two phases. In fact while in the hadron phase we have a large neutron potential repulsion (in particular in the  $NL\rho\delta$  case), in the quark phase we only have the much smaller kinetic contribution. Observables related to such neutron “trapping” could be an inversion in the trend of the formation of neutron rich fragments and/or of the  $\pi^-/\pi^+$ ,  $K^0/K^+$  yield ratios for reaction products coming from high density regions, i.e. with large transverse momenta.

From the above discussion and from the results reported in Section 6, it is clear that the possibility of a transition to the quark phase crucially depends on the way to describe the quark *EOS*. From this point of view, it appears extremely important to investigate the possible inclusion of the Isospin degree of freedom in the effective approaches to the QCD dynamics [40]. In fig.16 we report the *EOS* of symmetric and neutron matter for hadronic (full lines) and quark (dashed lines) phases. One can see that the transition to the quark phase is particularly convenient because, in the quark models considered so far, the symmetry energy of the quark matter takes contribution only from the kinetic energy and it is rather small. In fact, the two dashed lines in fig.16 are very close, while in the hadronic case the potential part of the symmetry energy is large.

Of course, these considerations are relevant also for the description of the properties of neutron stars.

## 8. Perspectives

We have reviewed some aspects of the rich phenomenology associated with nuclear reactions and astrophysical observations, from which interesting hints are emerging to constrain the nuclear EOS and, in particular, the largely debated density behavior of the symmetry energy. The greatest theoretical uncertainties concerns the high density domain, that has the largest impact on the understanding of the properties of neutron stars. This regime can be explored in terrestrial laboratories by using relativistic heavy ion collisions of charge asymmetric nuclei. Differential collective flows and meson production are promising observables. On the other hand, the behavior of the symmetry energy at low density can be accessed in reactions from low to intermediate energies, where collective excitations and fragmentation mechanisms are dominant. A considerable amount of work has already been done in this domain. In the near future, thanks to the availability of both stable and rare isotope beams, more selective analyses, also based on new exclusive observables, are expected to provide further stringent constraints.

## References

- [1] Danielewicz P, Lacey R and Lynch WG 2002 *Science* **298** 1592
- [2] Fuchs C, Wolter HH 2006 *Eur. Phys. Jour. A* **30** (2006)
- [3] Fantoni S *et al* 2008 *AIP Conf.Proc.* **1056** 233 and arXiv:0807.543[nucl-th].
- [4] Baldo M and Shaban AE 2008 *Phys. Lett. B* **661** 373
- [5] Li ZH, Lombardo U, Schulze H-J *et al* 2008 *Phys. Rev. C* **77** 034316
- [6] *Isospin Physics in Heavy-ion Collisions at Intermediate Energies*, Eds. Li BA and Schröder WU, Nova Science Publishers (2001, New York)
- [7] Baran V, Colonna M, Greco V, Di Toro M 2005 *Phys. Rep.* **410** 335.
- [8] Colonna M and Tsang MB 2006 *Eur. Phys. J A* **30** 165, and refs. therein.
- [9] Li BA, Chen LW, Ko CM 2008 *Phys. Rep.* **465** 113
- [10] Baldo M, Maieron C 2007 *J. Phys. G:Nucl. Part. Phys.* **34** R243; Baldo M *et al* 2004 *Nucl. Phys. A* **736** 241
- [11] Zhou XR, Burgio GF, Lombardo U, Schulze H-J, Zuo W 2004 *Phys. Rev. C* **69** 018801, and references therein.
- [12] Machleidt R 2001 *Phys. Rev. C* **63** 024001
- [13] Wiringa RB, Stoks VGJ, Schiavilla R 1995 *Phys. Rev. C* **51** 38
- [14] Carlson J, Pandharipande VR, Wiringa RB, 1983 *Nucl. Phys A* **401** 59
- [15] Li ZH, Lombardo U and Schulze H-J, submitted
- [16] Chomaz P, Colonna M, Randrup J 2004 *Phys. Rep.* **389** 263
- [17] Baran V *et al* 2002 *Nucl. Phys. A* **703** 603
- [18] Baran V *et al* 2005 *Phys.Rev. C* **72** 064620.
- [19] Baldo M, Maieron C 2008 *Physical Review C* **77** 015801
- [20] Tsang MB *et al* 2004 *Phys. Rev. Lett.* **92** 062701
- [21] Xu HS *et al* 2000 *Phys. Rev. Lett.* **85**, 716; Famiano *et al* *Phys. Rev. Lett.* **97** 052701; Igljo J *et al* 2006 *Phys. Rev. C* **74** 024605
- [22] Chomaz P, Di Toro M, Smerzi A 1993 *Nucl. Phys. A* **563** 509.
- [23] Pierroutsakou D *et al* 2005 *Phys. Rev. C* **71** 054605
- [24] Martin B, Pierroutsakou D *et al* (Medea Collab.) 2008 *Phys. Lett. B* **664** 47
- [25] Baran V, Brink DM, Colonna M, Di Toro M 2001 *Phys. Rev. Lett.* **87** 182501
- [26] Baran V, Rizzo C, Colonna M, Di Toro M, Pierroutsakou D 2009 *The Dynamical Dipole Mode in Fusion Reactions with Exotic Nuclear Beams*, arXiv:0807.4118[nucl-th]
- [27] Rizzo J *et al* 2008 *Nucl.Phys. A* **806** 79-104
- [28] Dasso CH, Gallardo MI, Lanza EG *et al* 2008 *Nucl. Phys. A* **801** 129
- [29] Li BA and Ko CM 1997 *Nucl.Phys. A* **618** 498
- [30] Bonasera A *et al* 2008 *Phys.Rev.Lett.* **101** 122702

- [31] Colonna M, Matera F 2008 *Physical Review C* **77** 064606
- [32] Colonna M *et al* 2008 *Phys. Rev. C* **78** 064618
- [33] De Filippo E *et al* (Chimera Collab.), *Time scales and isospin effects on reaction dynamics*, NN06 Conf., Rio de Janeiro, August 2006, and *Isospin signals in reaction dynamics*, Int.Conf.on Nuclear Fragmentation, Antalya 2007.
- [34] Di Toro M, Olmi A, Roy R 2006 *Eur. Phys. Jour.* **A30** 65
- [35] Li T, Garg U *et al* 2007 *Phys. Rev. Lett.* **99** 162503
- [36] Li BA, Das Champak B, Das Gupta S, Gale C 2004 *Nucl. Phys. A* **735** 563
- [37] Rizzo J, Colonna M, Di Toro M 2005 *Phys. Rev. C* **72** 064609.
- [38] Danielewicz P 2000 *Nucl. Phys. A* **673** 375
- [39] Giordano V, Master Thesis, Univ. of Catania 2008.
- [40] Di Toro M *et al* 2009 *Progress in Particle and Nuclear Physics*, doi:10.1016/j.ppnp.2008.12.038
- [41] Fuchs C, Wolter HH 1995 *Nucl. Phys. A* **589** 732.
- [42] G.Ferini, T.Gaitanos, M.Colonna, M.Di Toro, H.H.Wolter, *Phys. Rev. Lett.* **97** (2006) 202301.
- [43] Serot BD, Walecka JD 1986 *Advances in Nuclear Physics* **16** 1, eds. J. W. Negele, E. Vogt, (Plenum, N.Y.)
- [44] Fuchs C 2006 *Prog.Part.Nucl.Phys.* **56** 1
- [45] Peng GX, Li A, Lombardo U 2008 *Phys. Rev. C* **77** 065807
- [46] Nicotra OE, Baldo M, Burgio GF *et al* 2006 *Phys. Rev. D* **74** 123001
- [47] Landau LD, Lifshitz L, *Statistical Physics*, Pergamon Press, Oxford 1969.
- [48] Burgio GF, Plumari S 2008 *Phys. Rev. D* **77** 085022
- [49] Glendenning NK, Moszkowski SA 1991 *Phys. Rev. Lett.* **67** 2414
- [50] Di Toro M, Drago A, Gaitanos T, Greco V, Lavagno A 2006 *Nucl. Phys. A* **775** 102